

10. D. O. Burgess, M. J. Sharp, D. W. F. Mair, J. A. Dowdeswell, T. J. Benham, *J. Glaciol.* **51**, 219 (2005).
11. G. Kaser, J. G. Cogley, M. B. Dyurgerov, M. F. Meier, A. Ohmura, *Geophys. Res. Lett.* **33**, L19501 (2006).
12. M. F. Meier, A. Post, *J. Geophys. Res.* **92**, 9051 (1987).
13. M. B. Dyurgerov, M. F. Meier, *Occasional Paper No. 58*, (Institute of Arctic and Alpine Research, Univ. of Colorado, Boulder, CO, 2005).
14. We have revised the total area of GIC from  $785 \times 10^3$  km<sup>2</sup> to  $763 \times 10^3$  km<sup>2</sup> because of an overestimate of the glaciers peripheral to Greenland Ice Sheet. This adjustment has been applied throughout.
15. S. C. B. Raper, R. J. Braithwaite, *Nature* **439**, 311 (2006).
16. S. Rahmstorf, *Science* **315**, 368 (2007).
17. D. B. Bahr, M. F. Meier, *Water Resour. Res.* **36**, 495 (2000).
18. D. B. Bahr, *Water Resour. Res.* **33**, 1669 (1997).
19. Because there are many areas without complete inventories of GIC sizes, we used two estimation processes to fill gaps. First, we used an estimate of the probability of the number of glaciers greater than a certain area versus that area, based on percolation theory and on known size distribution relations. The error in this process for a global total was estimated at about 13% (13). Next, we estimated the thickness of GIC based on power-law scaling with glacier area. Without sufficient independent data, it is difficult to estimate the error in the method. We estimated that the error in calculating thicknesses and thus volumes from area values is on the order of 25% for global aggregates (13) but far greater, on the order of 50%, for individual ice masses.
20. M. F. Meier, D. B. Bahr, M. B. Dyurgerov, W. T. Pfeffer, *Geophys. Res. Lett.* **32**, L17501 (2005).
21. This work was supported by NSF grants OPP 0327345, OPP 0425488, and EAR 0549566; NASA grants NGT5-155 and NAG5-13691; and a Marie Curie International Fellowship within the 6th European Community Framework Program. We thank three anonymous reviewers for their critical reading of the manuscript.

### Supporting Online Material

www.sciencemag.org/cgi/content/full/1143906/DC1  
Figs. S1 to S3  
Table S1  
References

17 April 2007; accepted 10 July 2007  
Published online 19 July 2007;  
10.1126/science.1143906  
Include this information when citing this paper.

# The Southern Ocean Biological Response to Aeolian Iron Deposition

Nicolas Cassar,<sup>1\*</sup> Michael L. Bender,<sup>1</sup> Bruce A. Barnett,<sup>1</sup> Songmiao Fan,<sup>2</sup> Walter J. Moxim,<sup>2</sup> Hiram Levy II,<sup>2</sup> Bronte Tilbrook<sup>3</sup>

Biogeochemical rate processes in the Southern Ocean have an important impact on the global environment. Here, we summarize an extensive set of published and new data that establishes the pattern of gross primary production and net community production over large areas of the Southern Ocean. We compare these rates with model estimates of dissolved iron that is added to surface waters by aerosols. This comparison shows that net community production, which is comparable to export production, is proportional to modeled input of soluble iron in aerosols. Our results strengthen the evidence that the addition of aerosol iron fertilizes export production in the Southern Ocean. The data also show that aerosol iron input particularly enhances gross primary production over the large area of the Southern Ocean downwind of dry continental areas.

The rate of organic matter export from the surface waters of the Southern Ocean has an important impact on distributed properties of the environment. First, it influences the residual nutrient burden of waters that flow northward in the subsurface to supply nutrients to much of the extrapolar ocean (1). Second, carbon export removes CO<sub>2</sub> from surface waters, thereby influencing the atmospheric CO<sub>2</sub> concentration over both glacial-interglacial and anthropogenic time scales. There is compelling evidence that iron supply from a number of sources (such as coastal sediments, aerosols, upwelling, ice melting, and enhanced mixing over high topography) influences rates of both gross production and carbon export by Southern Ocean ecosystems. Ocean color data, for example, show that biomass is elevated downwind of aeolian iron sources, and extraordinary “patch” experiments have shown that iron addition enhances primary production

and new production in several representative regions (2).

To understand the potential for aeolian iron fertilization, we compared a large number of net community production (NCP) measurements in the Southern Ocean (3, 4) to a modeled Fe deposition (5). NCP and gross primary production (GPP) are calculated as the production rates required to maintain the observed biological O<sub>2</sub> supersaturation (derived from O<sub>2</sub>/Ar) and O<sub>2</sub> triple-isotope anomaly against equilibration by gas exchange (parameterized in terms of wind speed) (6). NCP from O<sub>2</sub> is the stoichiometrically equivalent rate of organic carbon production in excess of respiration; it approximates carbon export from the mixed layer. Our data set establishes the pattern of this fundamental rate process in the Southern Ocean at a scale heretofore accessed only for chlorophyll, which reflects biomass. We implemented these methods with samples of water from the upper-ocean mixed layer. Samples were collected by us or collaborators on cruises of opportunity and returned to the laboratory for analysis; in this way, it was possible to assemble a very large data set.

Our approach to determining NCP and GPP has distinct attributes and limitations. The method accesses production over times on the order of 1 week, corresponding to the mixed-layer depth divided by the piston velocity. We as-

sumed steady-state mixed-layer depth and productivity (clearly a simplification). We ignored exchange between the mixed-layer and underlying waters. The analysis of Wang *et al.* (7) suggests that, in the Polar Front Zone and the Subantarctic Zone, this process is of minor importance in the summer and in the spring. When the flux of O<sub>2</sub> is into the ocean, we report negative values of NCP. Although we refer to the air-sea biological O<sub>2</sub> flux as NCP, we were unable to determine whether negative values reflect net heterotrophy in the mixed layer or upwelling of O<sub>2</sub>-undersaturated waters.

Figure 1 shows summer NCP values superimposed on Southern Ocean properties (8). Most of the Southern Ocean can be considered a high-nutrient low-chlorophyll region, with the caveat that the area north of the Antarctic Polar Front (APF) is depleted in silicate during summertime. The strong westerlies around the Antarctic continent drive a northward Ekman transport of nutrient-rich circumpolar deep waters that upwell south of the APF. From the south, the Antarctic Zone lies between the Southern Boundary of the Antarctic circumpolar current and the APF, the Polar Frontal Zone stretches from the APF to the Subantarctic Front, and the Subantarctic Zone extends from the Subantarctic Front to the Subtropical Front. The Subtropical Front is the boundary between the warm and salty subtropical waters and the relatively cooler and fresher waters of the Southern Ocean. The summertime chlorophyll distribution is shown by the background colors of the map (Fig. 1).

We observed that, in general, NCP rises toward the north (Figs. 1 and 2), with considerable spatial heterogeneity. Visual inspection, along with the statistical analysis of Reuer *et al.* (4), shows that NCP is weakly correlated with climatological satellite chlorophyll estimates. Our results also show higher NCP and GPP in the spring than in the summer over most of the Southern Ocean (9) (Fig. 2). Our approach underestimates NCP in upwelling areas, where mixing to the surface of O<sub>2</sub>-depleted waters lowers the biological O<sub>2</sub> supersaturation. For this reason, the apparent poleward decrease in NCP could partially be driven by upwelling of upper circum-

<sup>1</sup>Department of Geosciences, Princeton University, Princeton, NJ 08544, USA. <sup>2</sup>Geophysical Fluid Dynamics Laboratory/National Oceanic and Atmospheric Administration, Post Office Box 308, Princeton, NJ 08542, USA. <sup>3</sup>Commonwealth Scientific and Industrial Research Organisation (CSIRO) Marine and Atmospheric Research and Antarctic Climate and Ecosystem Cooperative Research Center, Hobart, Tasmania 7001, Australia.

\*To whom correspondence should be addressed. E-mail: ncassar@princeton.edu

polar deep water south of the APF. However, we believe that part of this poleward decrease accurately reflects the gradient in mixed-layer fertility because chlorophyll concentration, as well as our  $^{17}\Delta$ -based estimates of GPP (which are less affected by upwelling), show a similar trend (Fig. 2).

We considered three properties that, individually and in combination, influence spatial variability of summertime Southern Ocean productivity:  $\text{Si(OH)}_4$ , light, and iron.  $\text{Si(OH)}_4$  undoubtedly limits diatom production at certain times but cannot account for the pattern of GPP and NCP that we observed: It is replete only in southern waters, but production is highest in the north (4). In addition, because of diatom Si:C plasticity, limitation of  $\text{Si(OH)}_4$  uptake does not necessarily entail carbon-specific growth limitation (10). The mixed layer is sometimes light-limited because deep mixed layers, with lower mean irradiance, are typical of the Southern Ocean. However, a comparison of our summer NCP measurements to climatological photosynthetically active radiation within the mixed layer shows no statistically significant correlation (fig. S1).

Iron might account for meridional variability in open ocean production in one of three ways. First, if the source of iron is upwelled subsurface waters, production should be elevated near the zone of upwelling—mainly around and south of the APF. Indeed, there is some evidence for higher production at the APF. However, as water upwells south of the APF and flows northward in the Ekman Drift, we do not observe the predicted decrease in production, which theoretically would be caused by removal of iron by scavenging and carbon export. Furthermore, studies from the Australian and Pacific sectors of the Southern Ocean agree that the mixed-layer Fe concentration increases, rather than decreases, toward the north (11–13). This iron increase to the north is accompanied by rising relative variable fluorescence as measured by fast repetition rate fluorometry (14, 15). Relative variable fluorescence is positively correlated to in situ Fe concentration in the Southern Ocean (14). In addition, phytoplankton communities north of the APF do not respond as strongly in Fe enrichment experiments as the ones south of the APF (15).

Second, if the source of iron is seasonal or annual aerosol input, production should be correlated to long-term average Fe deposition. Given a plausible residence time on the order of 5 months (calculated for the Subantarctic Zone assuming soluble iron deposition =  $0.06 \mu\text{mol m}^{-2} \text{day}^{-1}$ , mixed-layer depth = 30 m, and mixed-layer  $[\text{Fe}] = 0.3 \text{ nmol kg}^{-1}$ ), the dissolved Fe concentration will reflect aerosol deposition somewhat upstream of the sampling point, a complication we neglect here. In Fig. 3A, we plot NCP versus the annual iron deposition rate at the sampling location computed by Fan *et al.* (5). Their model, driven by analyzed meteorological properties, simulates chemical changes occurring in aerosols that increase Fe solubility with atmospheric transport time (Fig. 4A). This

increase in Fe solubility exerts a first-order control on aerosol Fe input to the oceans (16). Relative to a model assuming that a constant fraction of iron dissolves, models invoking chemical transformations predict diminished soluble Fe addition near dust sources and enhanced delivery in remote regions (Fig. 4B). Uncertainties in the entrainment rates of dust in the source areas and the fraction of soluble iron in settling aerosols introduce important errors into rates of soluble iron deposition simulated by the model. There is clearly a strong correlation between NCP and annual Fe deposition ( $r = 0.60$ ,  $\text{df} = 381$ ; Fig. 3A).

Third, if the source of iron is synoptic-scale deposition, production should be correlated with the deposition rate during some recent period. The correlation coefficient between NCP and soluble iron deposition is a maximum when iron deposition is averaged for a period of 14 days before sampling ( $r = 0.53$ ,  $\text{df} = 381$ ; Fig. 3B), decreasing only slightly with longer averaging times (6). This period may be shorter than the average residence time. Nevertheless, synoptic-scale events would lead to variability of about 25% in the ambient iron concentration given transient doublings and halvings of the soluble iron input with a 30-day cycling time. Such changes appear feasible based on the comparison of average Fe deposition at sampling sites during the 2-week period before collection and the average

annual Fe deposition at the sites (fig. S2), and the variability would of course be greater if the residence time were  $<5$  months. Fe excursions might raise NCP by inducing transient increases in phytoplankton growth that would eventually be curtailed as grazers respond. Alternatively, recently added iron might be more available to phytoplankton than iron that has resided for a longer time in the mixed layer. A large proportion of Fe in the mixed layer is organically chelated (17, 18), and the bioavailability of this ligand-complexed Fe is poorly understood (19). Similar analyses demonstrate the influence of soluble Fe deposition on GPP as well (fig. S3).

Thus, our data are compatible with either annual iron deposition or synoptic-scale iron deposition that has a significant influence on variability of NCP, as well as GPP, in the Southern Ocean. Statistical tests confirm the link between increasing iron deposition and increasing NCP and GPP (6). Some of the variability in NCP versus Fe deposition can be explained by other sources of Fe (such as meltwater, sedimentary, and upwelling sources), variable phytoplankton Fe:C quotas, light and silicate limitations, parameterization of the atmospheric Fe dissolution kinetics, aeolian transport model errors, and wind parameterization of the piston velocity.

To explore the potential and nature of atmospheric Fe fertilization, we performed a model

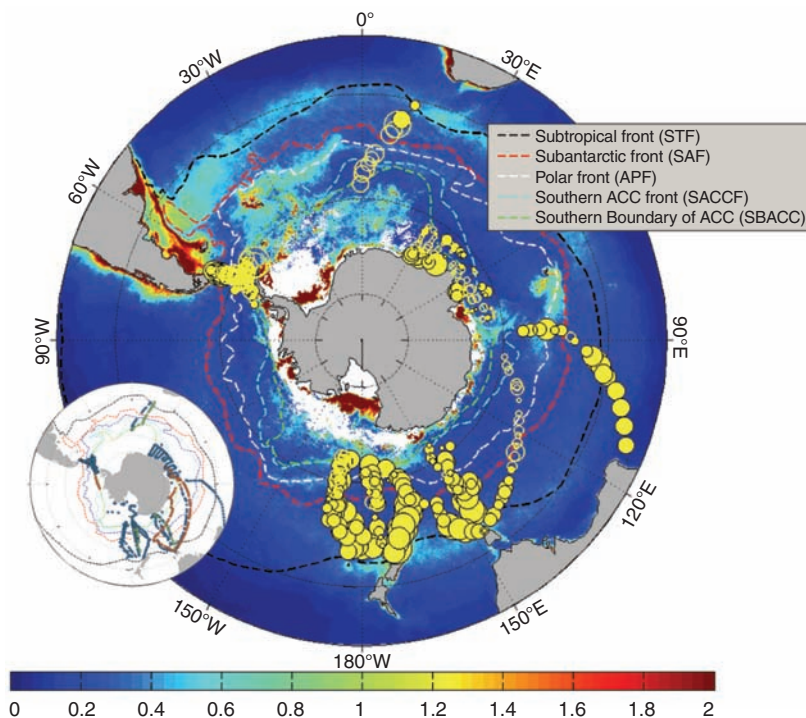


**Fig. 1.** Austral summer NCP measurements in the Southern Ocean. Yellow circles indicate locations of summertime  $\text{O}_2/\text{Ar}$  samples from which we calculated air-sea  $\text{O}_2$  fluxes and NCP values. Open circles denote  $\text{O}_2$ -undersaturated waters and  $\text{O}_2$  fluxes into the ocean. Closed circles reflect net autotrophy, with the circle size proportional to its magnitude. The largest filled circle represents  $168 \mu\text{mol O}_2 \text{ m}^{-2} \text{ day}^{-1}$ . Sea-Viewing Wide Field-of-View Sensor (SeaWiFS) summer chlorophyll a climatology is also shown (color bar, bottom, in  $\text{mg m}^{-3}$ ). (Inset) Color-coded sampling sites with summer, spring, and fall in blue, green, and orange, respectively. Dashed lines indicate the climatological locations of fronts that separate the main water masses associated with the Antarctic circumpolar current (ACC) (35).

II least-squares bisector regression analysis (20) to calculate the  $\text{Fe}/\text{C}_{\text{org}}$  ratio (aerosol Fe input/NCP) implied by our data (Fig. 3B). We adopted an  $\text{O}_2/\text{C}$  molar photosynthetic quotient of 1.4 for NCP (i.e., NCP is assumed to be mostly nitrate-derived) (21). The resulting  $\text{Fe}/\text{C}_{\text{org}}$  ratio for the spring and summer seasons is

$2.5 \mu\text{mol mol}^{-1}$ . This number is markedly similar to the oceanic Fe/C ratios in Southern Ocean phytoplankton (22) ( $1.5$  and  $2.1 \mu\text{mol mol}^{-1}$  in the Ross Sea and Drake Passage, respectively). For comparison, Fe:C in laboratory cultures of *Thalassiosira oceanica* varies between  $2.5$  to  $34 \mu\text{mol mol}^{-1}$  depending on Fe availability (23).

**Fig. 2.** Zonally averaged seasonal and regional gradient in (A)  $\text{O}_2/\text{Ar}$ -derived NCP, (B) oxygen triple isotope-derived GPP ( $\text{mmol m}^{-2} \text{day}^{-1}$ ) from available measurements, and (C) Fe deposition ( $\mu\text{mol m}^{-2} \text{year}^{-1}$ ) from corresponding model grid boxes. Standard error bars are also shown when available. STF, Subtropical Front; SAF, Subantarctic Front; PF, Antarctic Polar Front (APF); SACCF, Southern ACC Front; SBDY, southern boundary of the ACC.

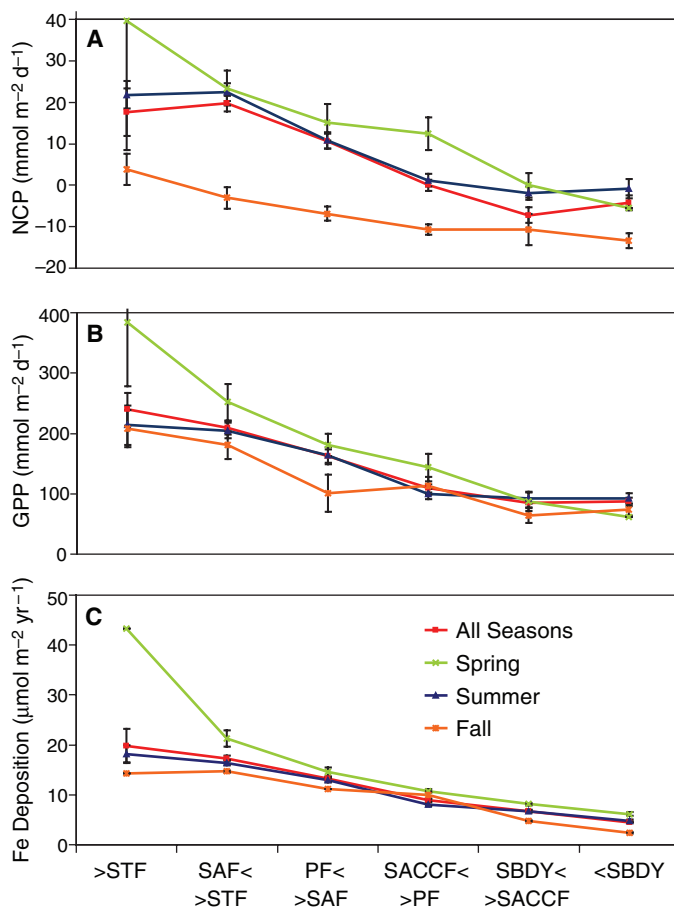
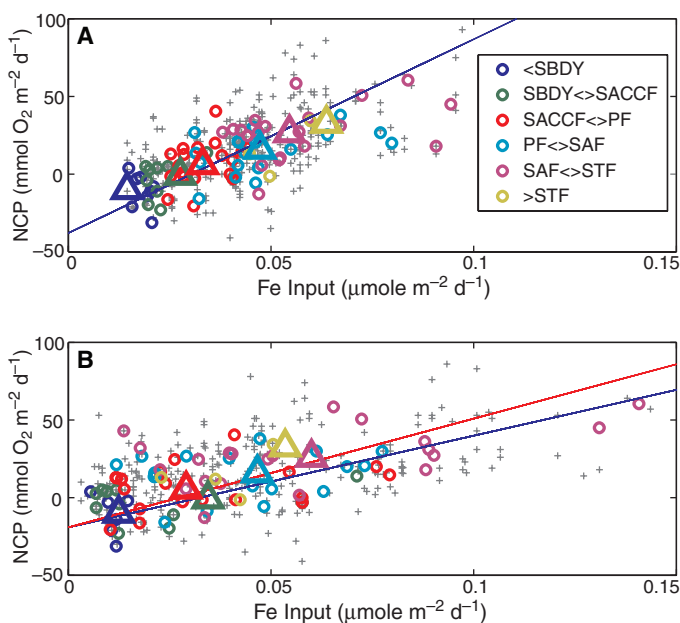


**Fig. 3.** Spring (16%) and summer (84%) NCP measurements versus corresponding modeled annual (A) and 2-week (B) Fe deposition rates. Gray pluses, circles, and triangles represent individual observations, regional averages for each transect, and regional averages of all samples, respectively. The blue line represents a model II least-squares bisector regression analysis. The red line represents an Fe requirement of  $1.4 \mu\text{M Fe}/\text{MO}_2$  [compatible with Sunda's (22) Southern Ocean phytoplankton's Fe:C ratio estimate and a photosynthetic quotient of 1.4 (21)].



In the Southern Ocean, where Fe is highly limiting, phytoplankton species are at the lower end of this range (24–28). Deriving our estimates for the cellular Fe quota based on NCP is reasonable if, in the mixed layer, Fe is stoichiometrically cycled along with organic carbon, rather than independently exported (28). Stoichiometric cycling is supported by the Fe/C remineralization ratio, which is also about  $2 \mu\text{mol mol}^{-1}$  (22). Hence, our results show that photoautotrophs may rely on aeolian input of Fe over a broad area of the Southern Ocean.

Our work, together with other recent studies, provides a comprehensive picture of the ways in which iron fertilization and iron limitation influence the biomass and fertility of Southern Ocean ecosystems. There are five sources of bioavailable iron to surface waters of the Southern Ocean. First, melting of sea ice can release accumulated iron that contributes locally to spring-time blooms along the ice edge (29). Second, the release of dissolved iron or resuspension of sediments can supply iron to waters overlying shallow sea floor, accounting for high productivity in continental shelf environments (along the Antarctic coast, for example) (30). Third, upwelling supplies iron and accounts for elevated productivity in some areas of the APF (31) and along the continental slope. Fourth, vertical mixing, induced by rough bottom topography, supplies iron to surface waters and enhances productivity in regions such as the Scotia Sea east of the Drake Passage, and the Kerguelen Plateau in the center of the Indian Antarctic sector (32). Finally, as we discuss, delivery of soluble iron by aerosol deposition supplies that element to the Southern Ocean, particularly areas downwind of substantial dust sources, accounting for elevated chlorophyll and/or productivity to the east of Patagonia and to the south and southwest of Australia, New Zealand, and Africa. Regions lacking all sources are the least fertile in the Southern Ocean, despite their high burdens of  $\text{NO}_3^-$ ,  $\text{PO}_4^{3-}$ , and  $\text{Si}(\text{OH})_4$ . These include waters overlying the Enderby Abyssal Plain (western Indian sector), South Indian Basin (eastern Indian sector), and the Bellingshausen abyssal Plain (Pacific sector), all in the Antarctic Zone of the Southern Ocean.

Both data and models support the idea that the flux of dust to the Southern Ocean was much higher during the last ice age than during the present or preindustrial times (33). In the Subantarctic region, lower  $\delta^{15}\text{N}$  of sedimentary nitrogen in glacial sediments (34), along with more rapid biogenic  $\text{SiO}_2$  accumulation, indicates higher rates of export production. Increased iron delivery is certainly a plausible explanation for faster export. According to the model of Robinson *et al.* (34), the resulting depletion of subantarctic waters in nutrients and  $\text{TCO}_2$  would have led to an atmospheric  $\text{CO}_2$  drawdown of up to 40 parts per million, accounting for nearly half the glacial lowering of atmospheric  $\text{CO}_2$ . Our work shows that delivery of

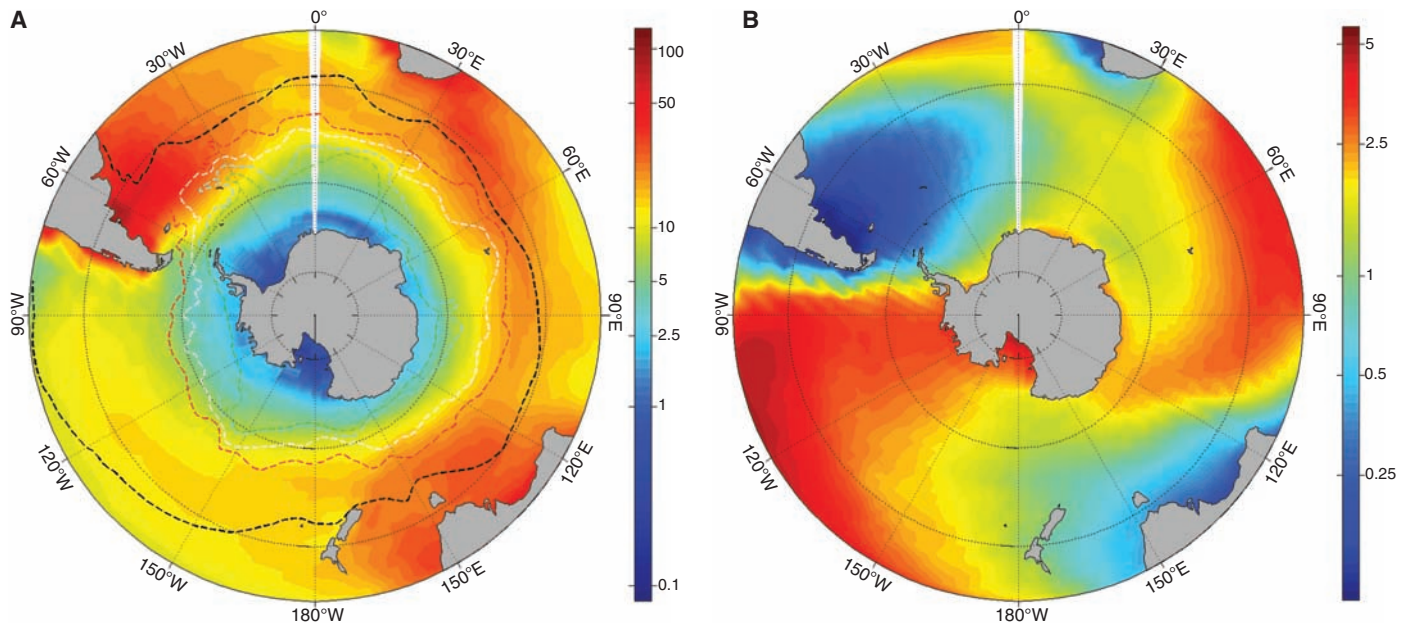


**Fig. 4.** (A) Annual deposition fluxes of dissolved Fe to the ocean based on the Fan *et al.* (5) two-step solubility process ( $\mu\text{mol m}^{-2} \text{year}^{-1}$ ). (B) Ratio of fluxes shown in (A) and a constant 5% Fe solubility model.

airborne Fe increases production of subantarctic waters, strengthening the link between enhanced Fe delivery and lower  $\text{CO}_2$  during the ice ages. Our work also underscores the importance of understanding the implications of the large change in dust transport to the ocean simulated for the coming centuries (33).

#### References and Notes

- J. L. Sarmiento, N. Gruber, M. A. Brzezinski, J. P. Dunne, *Nature* **427**, 56 (2004).
- P. W. Boyd *et al.*, *Science* **315**, 612 (2007).
- M. B. Hendricks, M. L. Bender, B. A. Barnett, *Deep-Sea Res. I* **51**, 1541 (2004).
- M. K. Reuer, B. A. Barnett, M. L. Bender, P. G. Falkowski, M. B. Hendricks, *Deep-Sea Res. I* **54**, 951 (2007).
- S. M. Fan, W. J. Moxim, H. Levy, *Geophys. Res. Lett.* **33**, L07602 (2006).
- Materials and methods are available as supporting material on Science Online.
- X. J. Wang, R. J. Matear, T. W. Trull, *J. Geophys. Res. Oceans* **106**, 31525 (2001).
- We include only springtime and summertime data in our discussion. Although fall data strengthen our conclusions, we omitted these results from our analysis because mixed-layer oxygen supersaturation can be influenced by entrainment of undersaturated subsurface waters.
- M. L. Dickson, J. Orcharo, *Deep-Sea Res. II* **48**, 4101 (2001).
- D. M. Nelson, M. A. Brzezinski, D. E. Sigmon, V. M. Franck, *Deep-Sea Res. II* **48**, 3973 (2001).
- P. N. Sedwick, P. R. Edwards, D. J. Mackey, F. B. Griffiths, J. S. Parslow, *Deep-Sea Res. I* **44**, 1239 (1997).
- H. J. W. de Baar *et al.*, *Mar. Chem.* **66**, 1 (1999).
- C. I. Measures, S. Vink, *Deep-Sea Res. II* **48**, 3913 (2001).
- H. M. Sosik, R. J. Olson, *Deep-Sea Res. I* **49**, 1195 (2002).
- M. R. Hiscock *et al.*, *Deep-Sea Res. II* **50**, 533 (2003).
- J. L. Hand *et al.*, *J. Geophys. Res.* **109**, D17205 (2004).
- E. L. Rue, K. W. Bruland, *Mar. Chem.* **50**, 117 (1995).
- J. F. Wu, G. W. Luther, *Mar. Chem.* **50**, 159 (1995).
- D. A. Hutchins, A. E. Witter, A. Butler, G. W. Luther, *Nature* **400**, 858 (1999).
- P. Sprent, G. R. Dolby, *Biometrics* **36**, 547 (1980).
- E. A. Laws, *Deep-Sea Res. A* **38**, 143 (1991).
- W. G. Sunda, *Mar. Chem.* **57**, 169 (1997).
- W. G. Sunda, S. A. Huntsman, *Mar. Chem.* **50**, 189 (1995).
- R. F. Strzepek *et al.*, *Global Biogeochem. Cycles* **19**, GB4526 (2005).
- B. S. Twining, S. B. Baines, N. S. Fisher, *Limnol. Oceanogr.* **49**, 2115 (2004).
- M. T. Maldonado *et al.*, *Limnol. Oceanogr.* **46**, 1802 (2001).
- W. G. Sunda, S. A. Huntsman, *Nature* **390**, 389 (1997).
- S. Blain *et al.*, *Nature* **446**, 1070 (2007).
- P. N. Sedwick, G. R. DiTullio, *Geophys. Res. Lett.* **24**, 2515 (1997).
- B. B. Prezelin, E. E. Hofmann, C. Mengelt, J. M. Klinck, *J. Mar. Res.* **58**, 165 (2000).
- H. J. W. Debaar *et al.*, *Nature* **373**, 412 (1995).
- E. Bucciarelli, S. Blain, P. Treguer, *Mar. Chem.* **73**, 21 (2001).
- N. M. Mahowald *et al.*, *J. Geophys. Res. Atmos.* **111**, D10202 (2006).
- R. S. Robinson *et al.*, *Paleoceanography* **20**, PA3003 (2005).
- A. H. Orsi, T. Whitworth, W. D. Nowlin, *Deep-Sea Res. I* **42**, 641 (1995).
- We thank P. Ginoux, M. Reuer, and P. Falkowski for helpful discussions, two anonymous reviewers for perceptive comments, and P. Schultz for providing the average climatological mixed layer PAR data-product. We gratefully acknowledge support for this work from NASA, NSF, the Gary Comer Family Foundation, and the CSIRO Climate Change Research Program.

#### Supporting Online Material

www.sciencemag.org/cgi/content/full/317/5841/1067/DC1

Materials and Methods

Figs. S1 to S4

Table S1

References

3 May 2007; accepted 20 July 2007

10.1126/science.1144602

## The Evolution of Selfing in *Arabidopsis thaliana*

Chunlao Tang,<sup>1</sup> Christopher Toomajian,<sup>1</sup> Susan Sherman-Broyles,<sup>2</sup> Vincent Plagnol,<sup>1,3</sup> Ya-Long Guo,<sup>4</sup> Tina T. Hu,<sup>1</sup> Richard M. Clark,<sup>4</sup> June B. Nasrallah,<sup>2</sup> Detlef Weigel,<sup>4,5</sup> Magnus Nordborg<sup>1\*</sup>

Unlike most of its close relatives, *Arabidopsis thaliana* is capable of self-pollination. In other members of the mustard family, outcrossing is ensured by the complex self-incompatibility (*S*) locus, which harbors multiple diverged specificity haplotypes that effectively prevent selfing. We investigated the role of the *S* locus in the evolution of and transition to selfing in *A. thaliana*. We found that the *S* locus of *A. thaliana* harbored considerable diversity, which is an apparent remnant of polymorphism in the outcrossing ancestor. Thus, the fixation of a single inactivated *S*-locus allele cannot have been a key step in the transition to selfing. An analysis of the genome-wide pattern of linkage disequilibrium suggests that selfing most likely evolved roughly a million years ago or more.

The transition from outcrossing to selfing is a major theme in the evolution of flowering plants, having occurred independently in numerous lineages (*1*). Although it leads to

inbreeding depression, the ability to self can be advantageous when colonizing new territory and is therefore associated with weedy and invasive species. *A. thaliana*, a member of the Brassicaceae,

# Comment on "The Southern Ocean Biological Response to Aeolian Iron Deposition"

Philip W. Boyd\* and Douglas Mackie

Cassar *et al.* (Reports, 24 August 2007, p. 1067) proposed that aerosol-iron input enhances Southern Ocean export production. Their conclusion critically depends upon aerosol-iron modeling simulations not validated with iron-deposition data and dust dissolution rates based on Northern Hemisphere atmospheric chemical conditions (low pH). This diminishes the relevance of their findings and demonstrates that applying such models to this region is premature.

Cassar *et al.* (1) reported that airborne delivery of iron associated with dust particles increases both primary and export production in Southern Ocean waters, with implications for alteration of atmospheric carbon dioxide concentrations, and hence global climate in both the geological past and the future. The authors used two distinctly different data sources to arrive at this conclusion: a large number of very accurate productivity observations in Southern Ocean waters based on either oxygen/argon samples or the oxygen triple isotope anomaly (whose limitations are identified and scrutinized), and model simulations of aerosol iron deposition (2). Although the productivity data set represents an important advance and valuable resource, we contend that it is mismatched with the aerosol-iron simulations (1, 2).

The Fan *et al.* model (2) should not be applied to the Southern Ocean for two important reasons. First, the aerosol solubility is based on atmospheric sulfur chemistry (1, 2), but the model parameterization [from (3)] is not described, and unrealistically low pH values (<2) are used to set aerosol dissolution. Such low aerosol pH values are only observed for dust plumes in Northern Hemisphere regions with high levels of atmospheric pollutants (4). Second, the published model predictions of global total input of both dust and soluble iron (2) were not validated with observations but only related to previous global model simulations (5).

In the Cassar *et al.* study (1), the model output was compared, without statistical analysis, with published aerosol iron dissolution estimates, mainly from the Northern Hemisphere (with only one aerosol sample from south of 45°S). Atmospheric sulfur concentrations, which affect dust dissolution (4), are much higher in the Northern Hemisphere compared with the rela-

tively pristine atmosphere above the Southern Ocean (3). In the supplementary information for (1), Cassar *et al.* compared predicted dust atmospheric concentrations with observations at three island sites ranging from Tasmania toward the pole, but acknowledged the absence of measurements of aerosol-iron supply to the Southern Ocean.

The conversion of dust deposition fluxes to those of oceanic iron supply currently represents a major challenge for ocean biogeochemists (6). Data are rare on dust deposition into Southern Ocean waters (7), and recent attempts to sample dust in this region revealed major technical issues such as high winds and seas (sea spray) and the need for longer sampling times to overcome the low aerosol deposition rates. Thus, Cassar *et al.*'s discussion of aeolian-iron deposition to these waters is based on data derived from an unvalidated model, which assumes low aerosol pH conditions for the Southern Hemisphere, and thus has poorly constrained links between the atmospheric sulfur (3) and iron dissolution (2) models.

Even if the described model (1, 2) was applicable to Southern Ocean waters, other important information from the emerging field of iron biogeochemistry was not considered by Cassar *et al.* (1), which raises questions about the validity of their conclusions. One of their central arguments for the importance of aerosol-iron deposition is the observed south-to-north increase in productivity. Cassar *et al.* argue that this cannot be driven by upwelled iron, which they suggest would be rapidly removed by scavenging and export. However, their argument ignores well-established trends from both lab culture (8) and field studies that phytoplankton take up high amounts of iron when it is readily available. This high iron uptake [termed "luxury uptake" (8)] ensures that cells remain iron-replete for several divisions and that high productivity can be maintained as phytoplankton are transported northward in this region. Such luxury iron uptake is likely responsible for the exceptional longevity of a polar mesoscale iron-enrichment (9) and may explain the presence of 2000-km-

long high chlorophyll plumes downstream of Southern Ocean islands such as South Georgia (10). These examples illustrate how biological responses to iron supply can complicate the identification of the relative importance of different iron supply mechanisms in these waters.

Problems in attributing the geographical influence of different iron supply mechanisms are further illustrated by Cassar *et al.*'s statement that high productivity is driven solely by dust supply downstream from Patagonia, Australia, New Zealand, and South Africa. The waters off New Zealand are characterized by the subtropical front [higher dissolved iron concentrations than subantarctic waters (7)], shallow shelf regions, and eddy activity, whose interactions, in addition to dust supply, play a key role in setting local productivity. Similar oceanic characteristics are evident east of Patagonia. Furthermore, there is little evidence, from an event-based analysis, of the biological impact of episodic dust storms in the waters south of both Australia and New Zealand (7).

Other recent findings from iron biogeochemistry negate the assumptions of Cassar *et al.*, including those centered on figure 3 in (1). For example, particulate iron has a deeper remineralization length scale than particulate organic carbon or nitrogen in the upper ocean (11, 12). Also, there is both direct (13) and indirect evidence (11) that oceanic microbes can access particulate iron, which suggests that aerosol solubility is only one component of particulate iron dissolution. Multiple time scales for surface mixed-layer iron dissolution have been proposed (12), from hours (physico-chemical mechanisms) to weeks (microbial/photochemical mechanisms). Such longer dissolution time scales, in conjunction with upper ocean physical transports, will also confound the attribution of the geographical extent of different iron supply mechanisms.

Although there is no doubt that dust supply plays an important role in oceanic iron supply (6, 12), the challenge is to determine the relative roles of both atmospheric and oceanic iron supply in the present, the geological past, and the future (14). Currently, there are insufficient data on atmospheric and oceanic iron supply, iron inventories, and the biogeochemical fate of iron. The Southern Ocean study of Cassar *et al.* (1) highlights many of these gaps in this region. A marked increase in data coverage on the above iron biogeochemical properties will be provided by new programs like GEOTRACES (15), with the subsequent development of more powerful iron biogeochemical models, parameterized and validated specifically for the Southern Ocean.

## References

1. N. Cassar *et al.*, *Science* **317**, 1067 (2007).
2. S. Fan, W. J. Moxim, H. Levy, *Geophys. Res. Lett.* **33**, L07602 (2006).
3. M. Chin *et al.*, *J. Geophys. Res.* **105**, 689 (2000).
4. N. Meskhidze, W. L. Chameides, A. Nenes, G. Chen, *Geophys. Res. Lett.* **30**, 2085 (2003).

National Institute of Water and Atmospheric Research Centre for Chemical and Physical Oceanography, Department of Chemistry, University of Otago, Dunedin, New Zealand.

\*To whom correspondence should be addressed. E-mail: pboyd@alkali.otago.ac.nz

5. N. Mahowald *et al.*, *Global Biogeochem. Cycles* **19**, GB4025 (2005).
6. T. D. Jickells *et al.*, *Science* **308**, 67 (2005).
7. P. W. Boyd, K. Richardson, V. Sherlock, M. Ellwood, R. D. Frew, *Global Biogeochem. Cycles* **18**, GB1029 (2004).
8. W. G. Sunda, S. A. Huntsman, *Mar. Chem.* **50**, 189 (1995).
9. E. R. Abraham *et al.*, *Nature* **407**, 727 (2000).
10. Ocean Color Web, [http://oceancolor.gsfc.nasa.gov/cgi/image\\_archive.cgi?c=CHLOROPHYLL](http://oceancolor.gsfc.nasa.gov/cgi/image_archive.cgi?c=CHLOROPHYLL).
11. R. D. Frew *et al.*, *Global Biogeochem. Cycles* **20**, GB1593 (2006).
12. P. W. Boyd *et al.*, *Global Biogeochem. Cycles* **19**, GB4520 (2005).
13. S. M. Kraemer, A. Butler, P. Borer, J. Cervini-Silva, *Rev. Mineral. Geochem* **59**, 53 (2005).
14. P. W. Boyd *et al.*, *Science* **315**, 612 (2007).
15. GEOTRACES, [www.ldeo.columbia.edu/res/pi/geotraces](http://www.ldeo.columbia.edu/res/pi/geotraces).

29 August 2007; accepted 10 December 2007  
10.1126/science.1149884

# Response to Comment on “The Southern Ocean Biological Response to Aeolian Iron Deposition”

Nicolas Cassar,<sup>1\*</sup> Michael L. Bender,<sup>1</sup> Bruce A. Barnett,<sup>1</sup> Songmiao Fan,<sup>2</sup> Walter J. Moxim,<sup>2</sup> Hiram Levy II,<sup>2</sup> Bronte Tilbrook<sup>3</sup>

Net community production in the Southern Ocean is correlated with simulated local dust deposition, and more so with modeled deposition of soluble iron. Model simulations of the latter two properties are consistent with observations in both hemispheres. These results provide strong evidence that aerosol iron deposition is a first-order control on net community production and export production over large areas of the Southern Ocean.

Our report (1) integrated data over large areas of the Southern Ocean and examined the relation between observed net community production (NCP) and simulated values of the rates of both dust deposition and soluble Fe deposition by dust. Dust and soluble Fe fluxes to the sea surface were simulated using a global three-dimensional atmospheric dust transport model (2) that accounts for Fe solubilization in aerosols (3). We observed a strong covariation between NCP and local values of soluble Fe deposition, with Fe/C ratio of  $2.5 \mu\text{mol mol}^{-1}$ , comparable to biological requirements. These results are consistent with aerosol Fe deposition rates exerting a first-order control on NCP.

Boyd and Mackie (4) argue that uncertainties in simulated soluble Fe in aerosols are so large that one cannot use simulated soluble Fe deposition rates to infer a link between this property and NCP. We disagree, but first circumvent the question of the soluble Fe fraction by simply comparing NCP with simulated dust deposition. As one approach, we average individual rates of spring and summer NCP and climatological dust deposition within each zone (i.e., area between fronts) for the Australian, New Zealand, and South American sectors of the Southern Ocean. We observe a strong correlation between NCP and dust deposition ( $r^2 = 0.65$ ,  $n = 15$ ), supporting our earlier conclusion that dust deposition is an important control on NCP in the Southern Ocean. If we assume that 3.5% of dust is Fe, and 5% of that Fe is soluble (5–7), the derived Fe/C of sinking organic matter is  $7.5 \mu\text{mol mol}^{-1}$ , again within the range of observations. Thus, a simple comparison between

dust flux and NCP supports the importance of dust fluxes.

When regressing NCP and simulated dust and soluble Fe values averaged for each zone of the entire Southern Ocean, both climatological dust and soluble Fe deposition explain a large proportion of NCP variability ( $r^2 = 0.69$  and  $0.98$ , respectively).

Although the processes involved in atmospheric Fe dissolution are still not fully understood (8, 9), the increase of Fe solubility with atmospheric transport time is now empirically well established (8, 10). Our model of atmospheric iron solubilization is consistent with Baker and Jickells' (8) empirical relationship of iron solubility versus dust content derived from North and South Atlantic Ocean measurements (fig. S1). Hence, our conclusions would be similar had we used an empirical relationship and made no assumption about the mechanism of iron solubilization (and aerosol pH) instead of using a prognostic model. Furthermore, observed Fe solubilities vary symmetrically on both sides of the equator and are therefore inconsistent with differing interhemispheric atmospheric Fe chemistry (11).

Contrary to Boyd and Mackie (4), we believe that our model of atmospheric surface coating of aerosols with  $\text{H}_2\text{SO}_4$ , followed by Fe dissolution, is appropriate in both hemispheres (see SOM text). This view is reinforced by the absence of correlation between atmospheric concentration of acid species and iron solubility (12, 13) (i.e., atmospheric acidity is saturating). Support comes from Luo *et al.* (9), who wrote that “in much of the atmosphere, cloud droplets may be acidic enough to process the iron, and that cloud processing is more important than predictions of acidity distributions.” Certainly,  $\text{H}_2\text{SO}_4$  from intense local pollution further enhances the acidity of aerosols (14).

Our modeled dust concentrations, dust deposition, and soluble Fe fraction in aerosols and precipitation are consistent with observations in the Southern and Northern Hemisphere [see table

S1 and (1–3)]. This consistency validates the Fan *et al.* (3) model for our purpose: the large-scale statistical comparison between NCP and simulated soluble iron deposition at more than 350 sampling points. The predictions of our dust entrainment and transport model are also consistent with other models (e.g., 15). To our knowledge, there are currently no direct observations of soluble Fe fluxes available for comparison to model predictions, and it seems unlikely that this property will be measured in the foreseeable future.

Boyd and Mackie assert that “there is little evidence, from an event-based analysis, of the biological impact of episodic dust storms in the waters south of both Australia and New Zealand.” We noted (1) that our data alone do not allow one to distinguish whether synoptic (episodic) events or seasonal inputs of dust are responsible for the link between aerosol supply of Fe and NCP. The dominance of wet over dry oceanic deposition of dust [as shown by observations and captured by atmospheric models (3, 16)] complicates the analysis of the biological response to episodic dust events. Episodic  $\text{CO}_2$  drawdowns and enhanced biological activity have been hypothesized to be triggered by dust events (17, 18). At the FeCycle site in the Subantarctic Zone southeast of New Zealand, Boyd *et al.* (19) conclude that the aeolian Fe supply is about 50 times as high as the oceanic supply of Fe.

Boyd and Mackie argue that the northward increase in NCP could be driven by “luxury uptake” (i.e., assimilation and storage of a non-limiting nutrient) of Fe south of the Antarctic polar front (APF) and by use of this stored Fe as phytoplankton are advected to the north. Several Fe enrichment experiments, both north and south of the APF, have demonstrated that the high-nutrient low-chlorophyll waters of the Southern Ocean are Fe limited (20). We agree that rapid zonal flows in the Southern Ocean produce chlorophyll plumes far downstream of island Fe sources (e.g., South Georgia). However, these results do not imply long-range northward transport by the slower meridional flows of the Ekman drift. Assuming northward transport of 38 Sv from upwelling around the APF (21) and a 40-m-deep mixed layer, the zonally averaged northward flow is around  $4 \text{ cm s}^{-1}$ . With a gross carbon specific growth rate of  $0.1 \text{ d}^{-1}$ , less than 5% of the original phytoplankton population at the APF remains 100 km to the north (e-folding of about 35 km). For comparison, our measurements extend equator-ward of the subtropical front, which sits, on average, more than 1600 km north of the APF (22). In addition, both Fe concentrations (23–25) and Fe sufficiency (26, 27) generally increase at latitudes north of the APF. Hence, Fe in biomass derived from upwelling at the polar front is an unlikely explanation for the northward increase in NCP.

Boyd and Mackie further assert that marine organisms strip additional lithogenic Fe from

<sup>1</sup>Department of Geosciences, Princeton University, Princeton, NJ 08544, USA. <sup>2</sup>Geophysical Fluid Dynamics Laboratory, National Oceanic and Atmospheric Administration, P.O. Box 308, Princeton, NJ 08542, USA. <sup>3</sup>Commonwealth Scientific and Industrial Research Organisation, Wealth from Oceans Flagship and Antarctic Climate and Ecosystem Cooperative Research Center, Hobart, Tasmania 7001, Australia.

\*To whom correspondence should be addressed. E-mail: ncassar@princeton.edu

dust (28). This process will substantially modify the stoichiometric relationship we envisioned but strengthens the link between dust and NCP. Their suggestion that continental shelves are important Fe sources to open ocean waters has merit, deserves further study, and can help account for our observation of high NCP at the northern bound of the Southern Ocean. However, recent evidence suggests that the meridional extent of shelves' impact on dissolved iron concentration could be limited (29). Any differences in remineralization depth scales between Fe and C are undoubtedly important but in no way negate our conclusions. Finally, we never claimed, and do not believe, that "high productivity is driven solely by dust supply downstream of Patagonia, Australia, New Zealand, and South Africa" (4).

We agree with Boyd and Mackie that there is a strong need for a better understanding of Fe biogeochemistry in the Southern Ocean through more extensive observations (including soluble fraction in aerosols, aerosol acidity, soluble Fe deposition from snow and rain, and surface ocean measurements) and improved and empirically tested atmospheric transport and oceanic biogeochemistry models. Several studies [cited in (1)] have clearly demonstrated that there are a multitude of Fe sources in the Southern Ocean.

Our study supports aerosol Fe as one important control on NCP over broad reaches of the Southern Ocean.

#### References and Notes

1. N. Cassar *et al.*, *Science* **317**, 1067 (2007).
2. S. M. Fan, L. W. Horowitz, H. Levy, W. J. Moxim, *Geophys. Res. Lett.* **31**, L02104 (2004).
3. S. M. Fan, W. J. Moxim, H. Levy, *Geophys. Res. Lett.* **33**, L07602 (2006).
4. P. W. Boyd, D. Mackie, *Science* **319**, 159 (2008); [www.sciencemag.org/cgi/content/full/319/5860/159a](http://www.sciencemag.org/cgi/content/full/319/5860/159a).
5. I. Y. Fung *et al.*, *Global Biogeochem. Cycles* **14**, 281 (2000).
6. J. K. Moore, S. C. Doney, K. Lindsay, *Global Biogeochem. Cycles* **18**, GB4028 (2004).
7. W. W. Gregg, P. Ginoux, P. S. Schopf, N. W. Casey, *Deep-Sea Res. II* **50**, 3143 (2003).
8. A. R. Baker, T. D. Jickells, *Geophys. Res. Lett.* **33**, L17608 (2006).
9. C. Luo *et al.*, *J. Geophys. Res. Atmos.* **110**, D23307 (2005).
10. Y. Chen, R. L. Siefert, *J. Geophys. Res. Atmos.* **109**, D09305 (2004).
11. A. R. Baker, M. French, K. L. Linge, *Geophys. Res. Lett.* **33**, L07805 (2006).
12. A. R. Baker, T. D. Jickells, M. Witt, K. L. Linge, *Mar. Chem.* **98**, 43 (2006).
13. J. L. Hand *et al.*, *J. Geophys. Res. Atmos.* **109**, D17205 (2004).
14. N. Meskhidze, W. L. Chameides, A. Nenes, G. Chen, *Geophys. Res. Lett.* **30**, 2085 (2003).
15. N. M. Mahowald *et al.*, *Global Biogeochem. Cycles* **19**, GB4025 (2005).
16. R. J. Kieber, K. Williams, J. D. Willey, S. Skrabal, G. B. Avery, *Mar. Chem.* **73**, 83 (2001).
17. E. Breviere, N. Metzl, A. Poisson, B. Tilbrook, *Tellus B* **58**, 438 (2006).
18. A. J. Gabric, R. Cropp, G. P. Ayers, G. McTainsh, R. Braddock, *Geophys. Res. Lett.* **29**, 1112 (2002).
19. P. W. Boyd *et al.*, *Global Biogeochem. Cycles* **19**, GB4520 (2005).
20. P. W. Boyd *et al.*, *Science* **315**, 612 (2007).
21. P. J. DiFiore *et al.*, *J. Geophys. Res. Oceans* **111**, C08016 (2006).
22. A. H. Orsi, T. Whitworth, W. D. Nowlin, *Deep-Sea Res. I* **42**, 641 (1995).
23. P. N. Sedwick, P. R. Edwards, D. J. Mackey, F. B. Griffiths, J. S. Parslow, *Deep-Sea Res. I* **44**, 1239 (1997).
24. H. J. W. de Baar *et al.*, *Mar. Chem.* **66**, 1 (1999).
25. C. I. Measures, S. Vink, *Deep-Sea Res. II* **48**, 3913 (2001).
26. H. M. Sosik, R. J. Olson, *Deep-Sea Res. I* **49**, 1195 (2002).
27. M. R. Hiscock *et al.*, *Deep-Sea Res. II* **50**, 533 (2003).
28. R. D. Frew *et al.*, *Global Biogeochem. Cycles* **20**, GB1593 (2006).
29. H. Planquette *et al.*, *Deep-Sea Res. II* **54**, 1999 (2007).
30. We are grateful to F. Morel (Princeton University) and A. Marchetti (University of Washington) for helpful discussions.

#### Supporting Online Material

[www.sciencemag.org/cgi/content/full/319/5860/159b/DC1](http://www.sciencemag.org/cgi/content/full/319/5860/159b/DC1)

SOM Text

Fig. S1

Table S1

References

1 October 2007; accepted 12 December 2007

10.1126/science.1150011